Eur. J. Mech., B/Fluids, **17,** n° 1, 19-31, 1998

Gravity flows with a free surface of finite extent

D. DABOUSSY *, F. DIAS * and J.-M. VANDEN-BROECK **

ABSTRACT. – Symmetric gravity flows bounded partly by rigid walls and partly by a free surface of finite extent are computed. It is shown that there are many different families of solutions. These flows can be viewed as generalizations of Richardson's, Riabouchinsky's, Roshko's and Joukovski's flows. Limiting configurations with stagnation points are obtained as well. © Elsevier, Paris.

1. Introduction

There are many two-dimensional flows which are bounded in part by solid plane walls and in part by a free surface of finite extent. These include Richardson's flow (*Fig.* 1 *a*), Joukovski's flow (*Fig.* 1 *b*), Riabouchinsky's flow (*Fig.* 1 *c*), Roshko's flow (*Fig.* 1 *d*) as well as the free-surface flows with two stagnation points of Vanden-Broeck and Dias (1996).

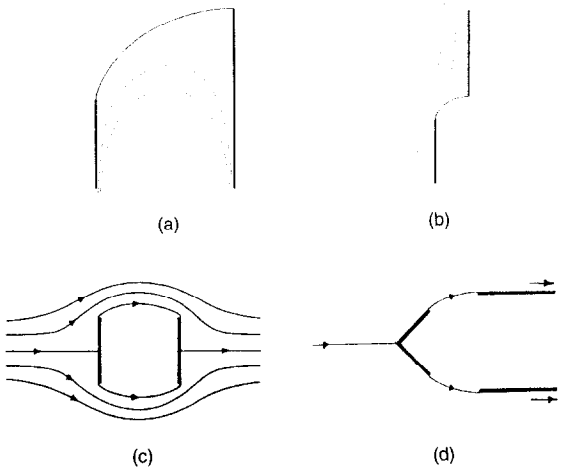

Fig. 1. – Examples of flows bounded in part by solid plane walls and in part by a free surface of finite extent: (a) Richardson's flow, (b) Joukovski's flow, (c) Riabouchinsky's flow, (d) Roshko's flow.

* Institut Non-Linéaire de Nice, UMR 6618–CNRS & UNSA, 1361, route des Lucioles, 06560 Valbonne, France.
** Department of Mathematics and Center for the Mathematical Sciences, University of Wisconsin-Madison, Madison, WI 53706, USA.

EUROPEAN JOURNAL OF MECHANICS, B/FLUIDS, VOL. 17, N° 1, 1998
0997-7546/98/01/© Elsevier, Paris

The Riabouchinsky's and the Roshko's flows were introduced as models for a cavity of finite extent and were calculated in the absence of gravity. For a detailed description of these models, one can refer to the original papers of Riabouchinsky (1921) and of Roshko (1955), or to the books by Birkhoff and Zarantonello (1957), Gurevich (1966) or Batchelor (1967).

The Joukovski's and the Richardson's flows were calculated by inverse methods (Joukovski, 1891; Richardson, 1920; Gurevich, 1966). They are free-surface flows in the presence of gravity which have the remarkable property that they can be described by explicit analytical solutions. Vanden-Broeck (1988) used Joukovski's solution as a model for a bubble rising in an unbounded fluid. He solved the problem numerically and showed that Joukovski's solution is just a particular solution of a one-parameter family of solutions.

The flows of Vanden-Broeck and Dias (1996) are also free-surface flows in the presence of gravity. These flows are related to the modelling of bow flows and were calculated numerically by boundary integral equation as well as series truncation methods. Many different branches of solutions were obtained.

The results of Vanden-Broeck (1988) and Vanden-Broeck and Dias (1996) suggest that many different interesting solutions should also exist for Riabouchinsky's flow if gravity is included. In this paper we investigate this question by considering a simplified configuration of a heavy fluid bounded in part by solid walls and in part by a free surface. A typical flow geometry is shown in Figure 2. The walls are semi infinite and make an angle α with the horizontal. Between the walls the boundary of the fluid is a free surface, whose position must be found as part of the solution.

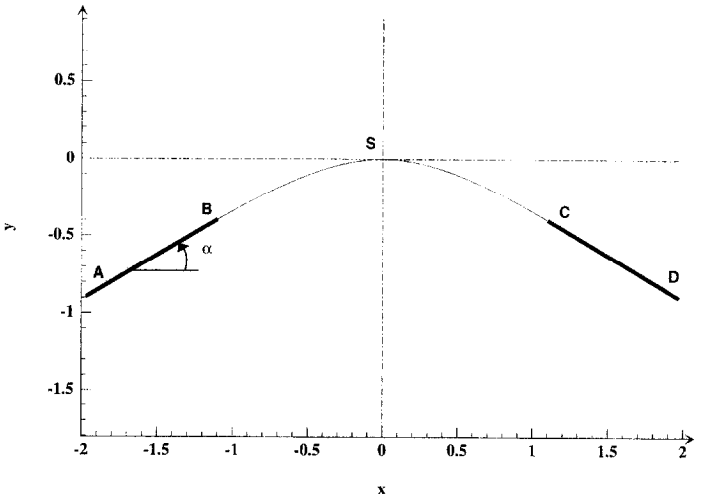

Fig. 2. – Sketch of the flow. Five points are labelled: the middle point of the free surface S, the ends of the walls B and C, and the points at infinity along the walls A and D. This is a computed solution with $\alpha = 30°$. The horizontal scale is the same as the vertical scale.

The problem is formulated in Section 2. A scheme based on series truncation is used to solve the problem numerically. Numerical results are described in Section 3

for horizontal as well as inclined walls. The angle α of the walls with the horizontal can vary between $-\pi/2$ and $\pi/2$. Limiting configurations are described in Section 4. In Section 5, we present some solutions with a free surface which exhibits several oscillations between the walls.

2. Formulation

The problem is formulated for symmetric flows. The generalization to asymmetric flows is described in a companion paper (Daboussy *et al.*, 1997). The flow configuration shown in Figure 2 is considered. The flow domain is bounded above by the walls AB and CD. The fluid is assumed to be incompressible and inviscid. The flow is assumed to be steady and irrotational. Far downstream and far upstream the velocity is infinite if $\alpha > 0$, uniform of value U if $\alpha = 0$, zero if $\alpha < 0$. We choose cartesian coordinates (X, Y) with the origin on the free surface halfway between the walls. The flow is assumed to be symmetric with respect to the Y-axis. The velocity potential ϕ and the stream function ψ are introduced. Without loss of generality we choose $\psi = 0$ on the free surface and $\phi = 0$ at the origin.

We define dimensionless variables by taking $(\phi_c^2/g)^{1/3}$ as unit length and $(\phi_c\, g)^{1/3}$ as unit velocity, where ϕ_c is the value of the potential a point C and g the acceleration due to gravity. The dimensionless coordinates are denoted by (x, y). The problem is then characterized by the dimensionless parameters

$$H = \frac{Y(S) - Y(B)}{(\phi_c^2/g)^{1/3}} = y(S) - y(B) = -y(B), \tag{2.1}$$

and

$$L = \frac{X(C) - X(B)}{(\phi_c^2/g)^{1/3}} = x(C) - x(B) = 2\,x(C). \tag{2.2}$$

H measures the dimensionless elevation of the middle point of the free surface above the ends of the walls (H is negative for flows with a hollow), while L measures the dimensionless width between the ends of the walls.

Next we define the complex velocity $\zeta = u - iv$, where u and v denote the horizontal and vertical components of the velocity. The function ζ is an analytic function of the complex potential $f = \phi + i\,\psi$ inside the flow domain. The flow configuration in the f-plane is shown in Figure 3. The free surface is described by $x(\phi)$ and $y(\phi)$. The values of $x(\phi)$ and of $y(\phi)$ can be evaluated in terms of u and v by integrating the identity

$$x_\phi + i y_\phi = \frac{1}{u - iv}. \tag{2.3}$$

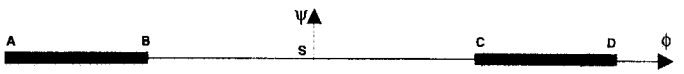

Fig. 3. – Sketch of the flow in the f-plane. The flow domain is the lower half plane. The images of the five points labelled in Figure 2 are shown.

On the free surface the pressure is constant. Therefore Bernoulli's equation yields

$$\frac{1}{2}(u^2+v^2)+y(\phi)=\text{Cte.} \tag{2.4}$$

The problem is to find ζ as an analytic function of f in the lower half plane $\psi<0$, satisfying Bernoulli's Eq. (2.4) on the free surface and the kinematic condition $v=u\tan\alpha$ along the walls. For horizontal walls, a physical quantity of interest is the pressure difference between the pressure at infinity p_{inf} along the walls and the atmospheric pressure p_{atm}. Let C_p define the pressure coefficient:

$$C_p=\frac{p_{\text{inf}}-p_{\text{atm}}}{\frac{1}{2}\rho U^2},$$

where U denotes the uniform velocity at infinity. The pressure coefficient can be expressed in terms of U and the velocity $U(B)$ by using Bernoulli's equation at infinity and at point B along the wall:

$$C_p=\frac{U^2(B)}{U^2}-1.$$

3. Numerical solutions

In this section we reformulate the problem in an intermediate plane. The flow domain is mapped onto the upper half unit disk and the complex velocity ζ is expanded as a Taylor series inside the unit disk after factoring out the singularities. The image of the free surface is the upper half unit circle. The image of the solid boundaries is the real diameter. The images of the five points A, B, S, C, D labelled in Figures 2 and 3 are $t=0$, $t=-1$, $t=i$, $t=+1$, $t=0$.

The mapping of the flow domain from the lower half plane of the complex potential (f-plane) to the upper half unit disk (t-plane) is provided by

$$f=\frac{1+t^2}{2t}. \tag{3.1}$$

The behaviour of the complex velocity at infinity is $\zeta\sim z^m$ where $2\alpha=\frac{m}{m+1}\pi$. It follows that $\zeta\sim t^{-2\alpha/\pi}$ as $t\to 0$. Next the complex velocity ζ is expanded as

$$\zeta=e^{i\alpha}t^{-2\alpha/\pi}\sum_{n=0}^{+\infty}a_n t^{2n}, \tag{3.2}$$

where the coefficients a_n are real.

The expansion takes advantage of the symmetry of the problem and of the singularity of the velocity at infinity, and satisfies the kinematic condition along the walls. Parameterizing the free surface by

$$t=e^{i\sigma},\qquad 0\le\sigma\le\pi/2,$$

and differentiating (2.4) with respect to σ leads to

$$u(\sigma)\,u_\sigma(\sigma) + v(\sigma)\,v_\sigma(\sigma) - \sin\sigma\,\frac{v(\sigma)}{u^2(\sigma)+v^2(\sigma)} = 0. \tag{3.3}$$

This completes the reformulation of the problem. The coefficients a_n in (3.2) are sought such that (3.3) is satisfied on the free surface.

The problem is solved numerically by truncating the infinite series in (3.2) after $(N-1)$ terms. Next we introduce the $(N-1)$ mesh points on the free surface

$$\sigma_I = \frac{I-\frac{1}{2}}{2(N-1)}\,\pi, \qquad I = 1, \ldots, N-1. \tag{3.4}$$

We satisfy the equation (3.3) at the mesh points (3.4). This yields $(N-1)$ equations for the following N unknowns: a_n, $n = 0, \ldots, N-1$. The last equation simply is $L = 2\,x(C)$ if L is specified, or $H = -y(B)$ if H is specified. For given values of L (or H) and α, this system of N nonlinear equations with N unknowns is solved by Newton's method.

The structure of the solutions turns out to be quite complicated. In order to understand this structure, it is natural to consider first the case when both walls are horizontal. Obviously, the solution with a horizontal free surface is always a solution for any spacing between the walls. The main result of this paper there is a discrete set of values L_n, $n = 1, 2, \ldots$, for the distance L between the walls at which bifurcations towards non-trivial solutions occur (the label L_n will be used to describe such bifurcated branches of solutions). The integer n denotes the number of oscillations for the small-amplitude bifurcated solutions. As n increases, the solutions have more and more oscillations. Intuitively, one sees that, as L increases, one can fit more and more waves between the walls. The case $n = 1$ corresponds to the simplest profiles, which have only one oscillation between the walls. Since the oscillation can be either a hump $(H > 0)$ or a hollow $(H < 0)$, the bifurcated branch crosses the L-axis in the (L, H)-plane. Recall that H denotes the amplitude of the solution at the origin. As the angle α becomes positive or negative, the bifurcations are perturbed. We begin our analysis of the solutions by considering the most intuitive perturbations: the perturbation of the solution with a hump as the angle α is increased from zero and the perturbation of the solution with a hollow as the angle α is decreased from zero.

The structure of these perturbed solutions as well as the bifurcated branch L_1 are shown in Figure 4. As said above, when $\alpha = 0$, one observes two types of solutions: solutions with a hump characterized by $H > 0$ and solutions with a hollow characterized by $H < 0$. Profiles are shown in Figure 5. The value of L_1 was found numerically to be equal to 2.80. One can find an approximation to this value with a simple argument. Realizing that this problem is close to the problem of periodic waves in deep water, we can write the wavelength of the wave in terms of the wave velocity by using the dispersion relation. With our choice of dimensionless variables, one gets

$$L_1 = 2\,\pi\,U^2.$$

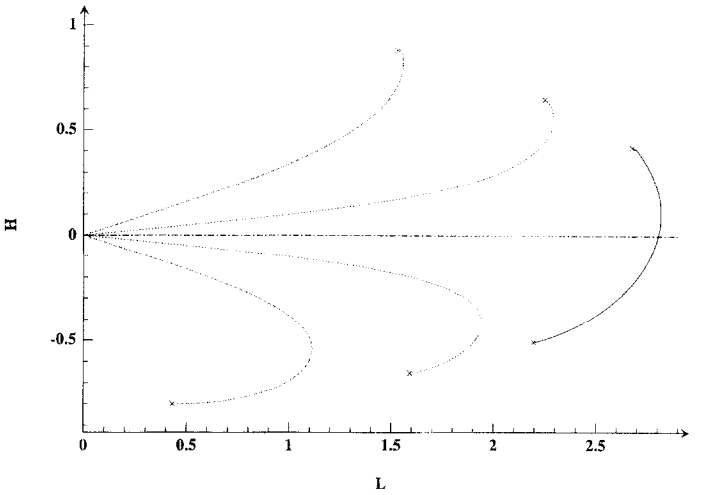

Fig. 4. – Branches of symmetric solutions: $\alpha = 0$ (solid line), $\alpha = 30°$ (small dotted line $H > 0$), $\alpha = -30°$ (small dotted line $H < 0$), $\alpha = 90°$ (large dotted line $H > 0$), $\alpha = -90°$ (large dotted line $H < 0$). When $\alpha = 0$, a branch bifurcates from a uniform flow when $L = 2.80$. The upper part of the branch represents solutions with a hump. The lower part of the branch represents solutions with a hollow. When $\alpha > 0$, the upper part of the branch persists but originates at 0. When $\alpha < 0$, the lower part of the branch persists but originates at 0. All branches end when the limiting configuration (120 degree crest for the upper branches, 120 degree departure from the walls for the lower branches) is reached. The crosses indicate these limiting profiles.

Moreover, since ϕ_c is the unit potential, one has

$$UL_1 = 2.$$

It follows that

$$L_1 = (8\pi)^{1/3} \sim 2.93, \tag{3.5}$$

in close agreement with the "exact" numerical value. Of course, the problem considered in this paper does not admit periodic solutions in x. Nevertheless the simple argument described above allows one to obtain a good approximation. Solving the linear problem exactly would provide the exact value of L_1 for the bifurcation to occur.

As explained above, we then perturbed the above solutions by considering inclined walls. Solutions were computed for all values of the angle between $-\pi/2$ and $+\pi/2$. We computed solutions with a hump for positive values of α and solutions with a hollow for negative values of α. Computed solutions are shown in Figures 2, 6 and 7. Solution branches for various angles are shown in Figure 4. Notice that the branches of solutions originate at the origin, as soon as the angle α is not equal to zero, and that, as a consequence, they lie to the left of the bifurcated branch L_1.

Then we asked ourselves whether the solution with a hump could also be perturbed for negative angles and whether the solution with a hollow could be perturbed for positive angles. Such solutions could be computed, at least for small values of the angle. They lie to the right of the bifurcated branch L_1. We show their relation with the solutions along the bifurcated branch L_2 in Section 5.

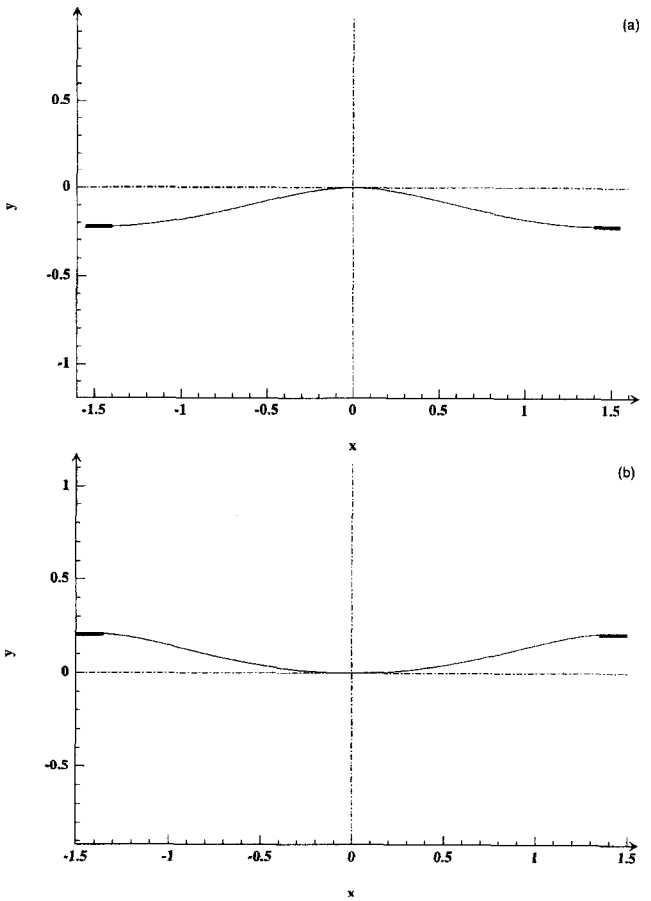

Fig. 5. – Computed solutions when the walls are horizontal. (a) Solution with a hump. The value of L is 2.80, the value of H is 0.22. The value of C_p is 0.27. (b) Solution with a hollow. The value of L is 2.70, the value of H is -0.20. The value of C_p is -0.34.

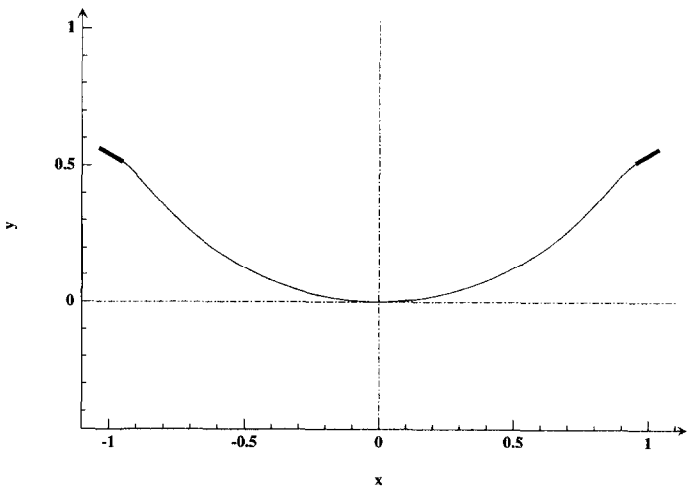

Fig. 6. – Computed solution with $H = -0.51$, $L = 1.90$ and $\alpha = -30°$.

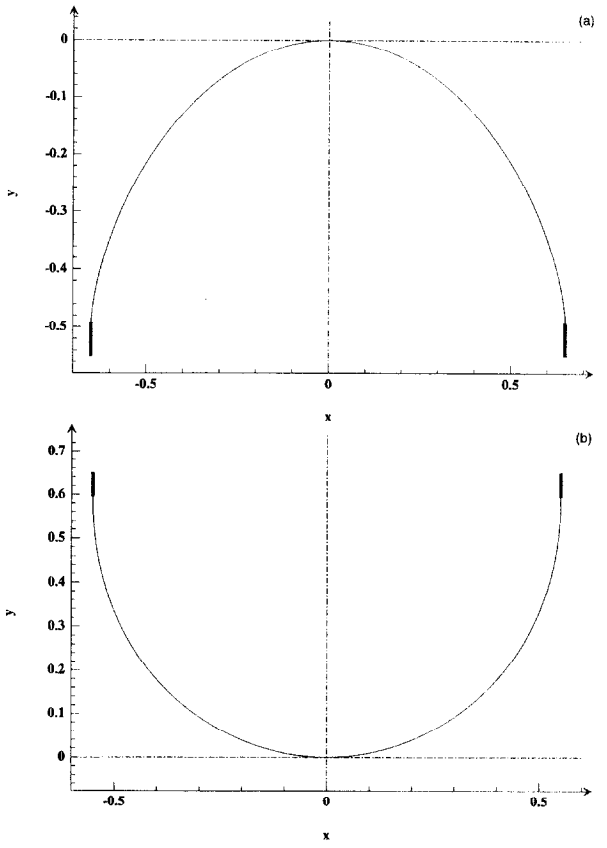

Fig. 7. – (a) Computed solution with $\alpha = 90°$, $H = 0.49$, $L = 1.30$.
(b) Computed solution with $\alpha = -90°$, $H = -0.60$, $L = 1.10$.

4. Limiting configurations

Before we consider more complicated solutions, we study the limiting configurations which occur along the branches of solutions described in the previous section. The branches of solutions with $H > 0$ end where the free surface reaches a limiting profile with a 120° angle at the crest. The branches of solutions with $H < 0$ end where the free surface leaves the walls with two 120° angles, one at B and the other at C.

The previous expansions for the velocity can be modified in order to include the limiting configurations. They become

$$\zeta = e^{i\alpha}\,(1+t^2)^{1/3}\,t^{-2\alpha/\pi}\sum_{n=0}^{+\infty} a_n\,t^{2n}, \tag{4.1}$$

for the solutions with a hump, and

$$\zeta = e^{i\alpha}\,(1-t^2)^{2/3}\,t^{-2\alpha/\pi}\sum_{n=0}^{+\infty} a_n\,t^{2n}, \tag{4.2}$$

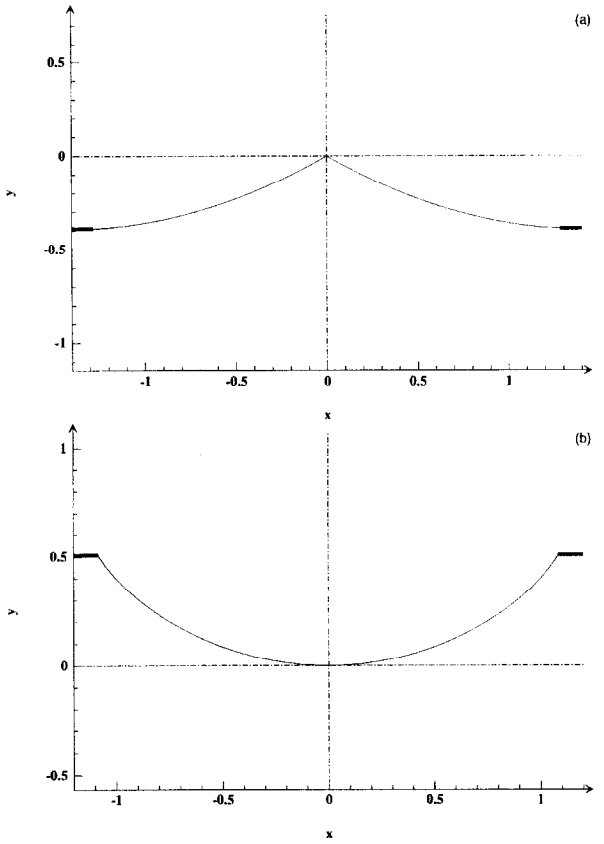

Fig. 8. – Limiting profiles for α=0. (a) Solution with a hump. The computed values are H=0.42, L=2.67. (b) Solution with a hollow. The computed values are $H = -0.51$, $L = 2.19$.

for the solutions with a hollow. Computed profiles for several values of the angle α are shown in Figures 8 and 9. The corresponding solutions are indicated by crosses in the bifurcation diagram of Figure 4.

5. Flows with several oscillations

As said above, the solutions described above are only part of the rich set of solutions. There are also solutions characterized by several oscillations between the walls. Such solutions can be obtained with the same computer program, with different initial guesses. Obviously, they lie to the right of the branch L_1 in the (L, H)-plane. When the angle α is equal to zero, the next branch to investigate is the branch L_2, which corresponds to solutions with two oscillations between the walls. Such solutions are shown in Figure 10. As opposed to the branch L_1, the solutions with humps are characterized by a negative value of H while the solutions with hollows are characterized by a positive value of H. In fact, H no longer is a good parameter to describe the solutions because H is close to zero for all solutions on the branch L_2. However, we still use H as a parameter in order to make the connection with the solution of Section 3.

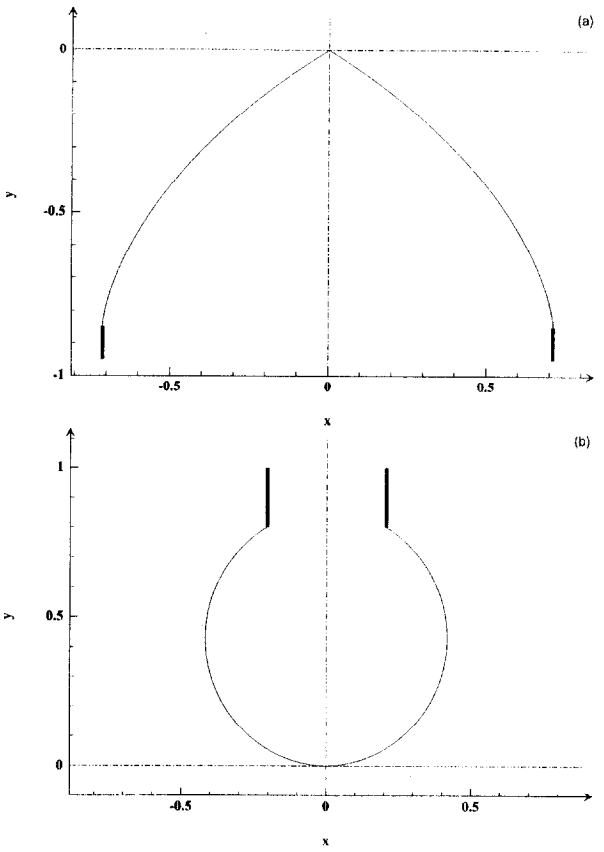

Fig. 9. – Limiting profiles for $\alpha=\pm 90^{\circ}$. (a) Solution with a hump. The computed values are $H=0.88$, $L=1.53$. The flow is inside the bubble. (b) Solution with a hollow. The computed values are $H=-0.80$, $L=0.43$. The flow is outside the bubble.

We were able to detect the bifurcation L_2 numerically and the bifurcated branch L_2 is shown in Figure 11. The bifurcation occurs at $L_2 = 3.61$. Again, the same straightforward argument as the one used in Section 3 leads to $L_2 = (16\,\pi)^{1/3} \sim 3.69$, in closer agreement with the "exact" numerical value. This argument will provide a better and better approximation as the number of oscillations increases.

Let us now perturb the branch L_2 for nonzero values of the angle α. The "natural" way to perturb the solutions with two hollows (*Fig.* 10*a*) is to consider negative values of α, while the natural way to perturb the solutions with two humps (*Fig.* 10*b*) is to consider positive values of α. By doing so, we obtained additional branches of solutions lying to the left of the branch L_2 and to the right of the branch L_1. Recall that at the end of Section 3 we asked ourselves whether the solutions with one hump could be perturbed for negative angles and whether the solutions with one hollow could be perturbed for positive angles. It turns out that when α is negative the solutions with one hump and the solutions with two hollows lie on the same branch and that one can go continuously from one to the other. When α is positive the solutions with one hollow and the solutions

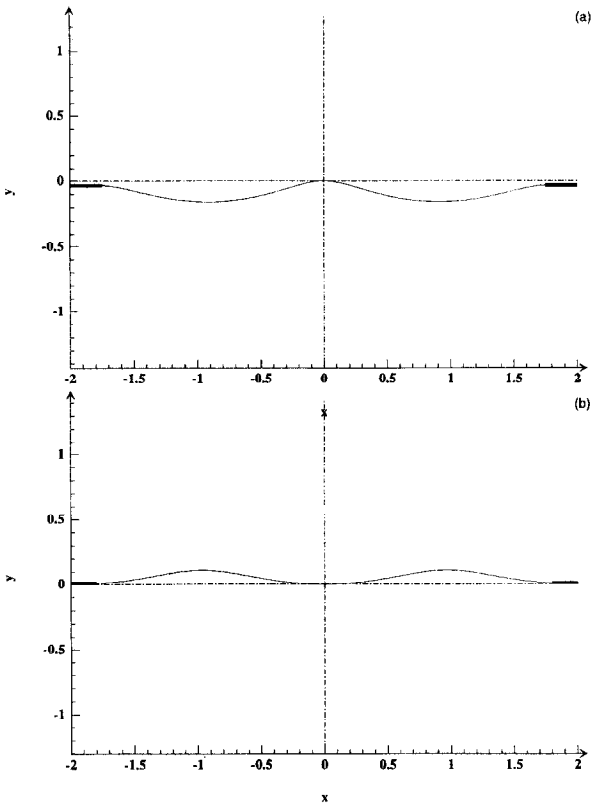

Fig. 10. – (a) Computed solution with two oscillations, with $\alpha = 0$, $H = 0.034$, $L = 3.50$.
(b) Computed solution with two oscillations, with $\alpha = 0$, $H = -0.01$, $L = 3.59$.

with two humps also lie on the same branch and one can go continuously from one to the other. This is illustrated on Figure 11.

What about the limiting configurations along these new branches? Let us first consider the branch L_2. The upper part of the branch L_2 ends where the free surface reaches a limiting profile with a 120° angle at the central crest while the lower part ends where the free surface exhibits two 120° angles on the free surface. The limiting configurations of the upper and of the lower parts of the branch have been computed and are shown by crosses in the bifurcation diagram (*Fig.* 11). Note that the limiting configuration of the lower part requires some changes in the numerical scheme since the location of the 120° singularities is unknown (Vanden-Broeck and Dias, 1996).

Let us now consider the limiting configurations along the branches with nonzero angles. Both end points of the branch of solutions for $\alpha = -5^\circ$ correspond to profiles with a 120° angle at the central crest. Both are shown by crosses in the bifurcation diagram of Figure 11. The branch of solutions for $\alpha = +5^\circ$ ends on the left (recall that on the left of the branch the solution is characterized by a single hollow) where the free surface leaves the walls with two 120° angles, one at B an the other at C, and on the right (recall that on the right of the branch the solution is characterized by two humps) with a limiting profile with two 120° angles on the free surface. The limiting profiles on the

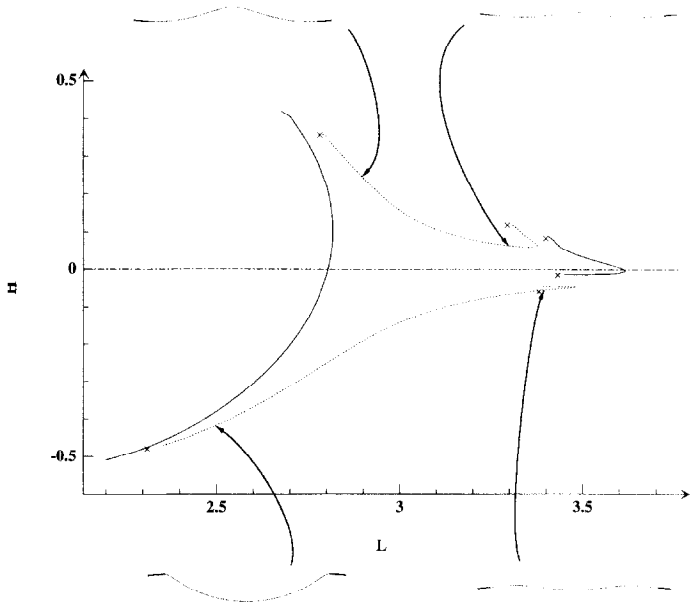

Fig. 11. – Additional branches of solutions. The branch on the left (solid line, $\alpha = 0$) is the same as the branch on the right of Figure 4. The branch on the right (solid line) is the branch of solutions with two oscillations ($\alpha = 0$). This branch bifurcates from a uniform flow when $L = 3.61$. It has two parts: solutions with two hollows ($H > 0$) and solutions with two humps ($H < 0$). The other branches (dotted lines) connect the branch of solutions with one oscillation to the branch of solutions with two oscillations. The upper one is for $\alpha = -5^{\circ}$ and the lower one if for $\alpha = 5^{\circ}$. Profiles along these branches show the transition. The crosses indicate the limiting profiles.

left as well as on the right of the branch have been computed and are shown by crosses in the bifurcation diagram of Figure 11. Again the limiting configuration on the right of the branch requires some changes in the numerical scheme since the location of the 120° singularities is unknown.

All the solutions described in this section were obtained for small values of $|\alpha|$. What happens as $|\alpha|$ increases remains an open problem. However, in our companion paper on asymmetric solutions, we show that certain solutions can disappear as the angle α goes beyond a threshold.

A generalization of the previous branches of solutions to higher values of n can be done. One expects to have branches of solutions starting on the right of the branch L_n and going towards the left of the branch L_{n+1}.

Acknowledgement

The computations presented in this work were performed on the CRAY C90 vector supercomputer located at IDRIS (Institut du Développement et des Ressources en Informatique Scientifique, France), and were funded by CNRS (Centre National de la Recherche Scientifique).

REFERENCES

BATCHELOR G. K., 1967, *An introduction to fluid dynamics*, Cambridge University Press.
BIRKHOFF G., ZARANTONELLO E. H., 1957, Jets, wakes and cavities, *Appl. Math. Mech.*, **2**, Academic Press.

DABOUSSY D., DIAS F., VANDEN-BROECK J.-M., 1997, On explicit solutions of the free-surface Euler equations in the presence of gravity, *Phys. Fluids.*, **9**.

GUREVICH M. I., 1966, *The theory of jets in an ideal fluid*, Pergamon Press.

JOUKOVSKI N. W., 1891, *J. Russian Physico. Chem. Soc.*, **22**, 19.

RIABOUCHINSKY D., 1921, On steady fluid motions with free surfaces, *Proc. London Math. Soc. II*, **19**, 206-215.

RICHARDSON A. R., 1920, Stationary waves in water, *Phil. Mag.*, **40**, 97-110.

ROSHKO A., 1955, On the wake and drag of bluff bodies, *J. of the Aeronaut. Sciences*, **22**, 124-132.

VANDEN-BROECK J.-M., 1988, Joukovski's model for a rising bubble, *Phys. Fluids*, **31**, 974-977.

VANDEN-BROECK J.-M., DIAS F., 1996, Free-surface flows with several stagnation points, *J. Fluid Mech.*, **324**, 393-406.

(Manuscript received December 4, 1996;
revised June 12, 1997;
accepted June 25, 1997.)